Phase diagram of uniaxial liquid crystals

1994 J. Phys. A: Math. Gen. 27 L771

(http://iopscience.iop.org/0305-4470/27/20/003)

J. Phys. A: Math. Gen. 27 (1994) L771–L776. Printed in the UK

LETTER TO THE EDITOR

Phase diagram of uniaxial liquid crystals

Giuseppe Gonnella†, Amos Maritan‡ and Jayanth R Banavar§

† Dipartimento di Fisica dell'Università di Bari and Istituto Nazionale di Fisica Nucleare, Sezione di Bari via Amendola 173, I-70126 Bari, Italy

‡ Dipartimento di Fisica Galileo Galilei and Istituto Nazionale di Fisica Nucleare, Sezione di Padova via F Marzolo 8, 35131 Padova, Italy

§ Department of Physics and Center for Materials Physics, The Pennsylvania State University, 104 Davey Laboratory, University Park, PA 16802, USA

Received 20 June 1994

Abstract. The phase diagram of an n-component spin model with dipolar and quadrupolar nearest-neighbour interactions is solved exactly in the large-n limit. In $d = 3$ a tricritical point is found on the line bounding the paramagnetic phase, at which the first-order transition becomes continuous at decreasing values of the quadrupolar exchange energy. In $d = 2$ the line of first-order transition ends at a critical point. The nematic–ferromagnetic transition is studied at order $1/n$.

The principal goal of this letter is to report the results of an analytic study of the $n \to \infty$ limit of a spin model defined by the Hamiltonian

$$\mathcal{H} = -\beta^{-1} \sum_{\langle ij \rangle} \left[J_1 S_i \cdot S_j + J_2 (S_i \cdot S_j)^2 \right] \tag{1}$$

where $\beta^{-1} = K_B T$, the sum is over the nearest neighbours in a d-dimensional hypercubic lattice and $S_i = (S_i^1, \ldots, S_i^n)$ is a unit vector at the i-site. This model was introduced by Krieger and James [1] to describe successive orientational transitions in molecular crystals. At $J_1 = 0$ the model reduces to the Maier–Saupe model [2] describing the nematic–isotropic transition in liquid crystals, while at $J_2 = 0$, it is the familiar classical Heisenberg model. For both $J_1 \neq 0$ and $J_2 \neq 0$, it describes uniaxial liquid crystals in which ferroelectric or antiferroelectric ordering is possible [3, 4]. Such a model has also been proposed for the interactions between Mn^{2+} ions in MgO doped with Manganese [5]. The J_2 coefficient is found to be large in situations where the orbital motion is not quenched and a pseudo-spin formalism is used to characterize the energy levels. Finally, we observe that the model (1) is equivalent to the Ising gauge model coupled to classical spin matter [6] in the limit of large gauge couplings, so that the behaviour of (1) is relevant to the description of the phase diagram of that gauge model.

An exact solution of the model (1) is known in $d = 1$ [7], while, more generally, the phase diagram is known in mean-field approximation [1]. A qualitative description of the phase diagram, at least at positive J_2, can easily be given. First, one observes that the phase diagram at negative J_1 is the antiferromagnetic counterpart of the one at positive J_1. At large values of J_2, parallel or antiparallel spin configurations are favoured, so that, if the RP^{n-1} invariance [8] is broken, on varying J_1 at low temperatures, an Ising-like transition

0305-4470/94/200771+06$19.50

is expected between a phase with oriented spins (ferromagnetic), and a phase with nematic ordering. At $J_2 = 0$, for $d > 2$, one has a continuous transition of the n-component classical Heisenberg model between the isotropic and the ferromagnetic phase. Therefore, at positive J_1 and J_2, three phases are expected: a high-temperature paramagnetic phase bounding a nematic phase at large J_2 and small J_1, and a ferromagnetic phase at large J_1. This is just the picture emerging from the mean-field calculation of [1], confirmed by numerical simulations [4]. Less clear is the situation at negative J_2, where there is competition between the two terms in (1). It is known only that at $d = 1$ for $J_2 < -J_1/2$ there is no long-range order even at $T = 0$ [7]. At a generic dimension, mean-field results of [1] give a continuous transition at $J_1 = 3/2d$, with a disordered phase extending to $T = 0$.

Here we will study the phase diagram of model (1) in the limit of large n. In this limit at $J_2 = 0$ the model is equivalent to the spherical model [9, 10] with the well known continuous transition with an upper critical dimension $d_c = 4$. With $J_1 = 0$, it has been studied in [8, 11] and a first-order transition has been found for integer $d \geqslant 2$. We now study the large-n limit for arbitrary J_1 and J_2.

We consider the partition function

$$\mathcal{Z} = \int_{-\infty}^{+\infty} \prod_i \mathrm{d}S_i^1 \ldots \mathrm{d}S_i^n \delta\left(\frac{S_i^2}{n} - 1\right) \mathrm{e}^{J_1 \sum_{\langle ij \rangle} S_i \cdot S_j + J_2/n \sum_{\langle ij \rangle} (S_i \cdot S_j)^2} \tag{2}$$

where the couplings have been rescaled in order to get a sensible $n \to \infty$ limit. As usual, the contraints in the integral (2) can be recast by introducing the standard δ-function representation

$$\delta\left(\frac{S_i^2}{n} - 1\right) = \frac{n}{2\pi} \int_{-\mathrm{i}\infty}^{\mathrm{i}\infty} \mathrm{e}^{-nz_i (S_i^2/n - 1)} \, \mathrm{d}z_i \tag{3}$$

where the integral is in the complex plane with $\mathrm{Re}\, z$ arbitrary. Moreover, the biquadratic term in the Hamiltonian can be expressed as

$$\mathrm{e}^{(J_2/n)(S_i \cdot S_j)^2} = \sqrt{\frac{n}{4\pi |J_2|}} \int \mathrm{d}A_{ij} \, \mathrm{e}^{-nA_{ij}^2/4J_2 + A_{ij} S_i \cdot S_j} \tag{4}$$

where the integral is on the real axis if $J_2 > 0$ and on the imaginary axis with arbitrary $\mathrm{Re}\, A_{ij}$ if $J_2 < 0$. Therefore, the partition function can be written

$$\mathcal{Z} = \left(\sqrt{\frac{n}{4\pi |J_2|}}\right)^{dN} \left(\frac{n}{2\pi}\right)^N \int_{-\mathrm{i}\infty}^{\mathrm{i}\infty} \prod_i \mathrm{d}z_i \int \prod_{\langle ij \rangle} \mathrm{d}A_{ij} \, \mathrm{e}^{n\left[\sum_i z_i - \sum_{\langle ij \rangle} A_{ij}^2/4J_2 - Nf_0\right]} \tag{5}$$

where e^{-Nnf_0} is the result of the Gaussian integration over the variables S_i. In the $n \to \infty$ limit the partition function can be evaluated by the steepest-descent method, with the free energy per site and per component $f \equiv -\ln \mathcal{Z}/Nn$ given by the quantity in square brackets in (5). Looking for homogeneous solutions $z = z_i \forall i$ and $A_{ij} = A \forall \langle ij \rangle$ of the saddle-point equations $\partial f/\partial z = 0$ and $\partial f/\partial A = 0$, the free energy reads as

$$f = \frac{1}{2N} \sum_q \ln\left[z - (A + J_1) \sum_{\mu=1}^{d} \cos q^\mu\right] - \tfrac{1}{2} \ln \pi + z - d\frac{A^2}{4J_2} \tag{6}$$

where the sum is over the first Brillouin zone in the reciprocal lattice. On defining the new variables $\Lambda = 2A$, $\Lambda_1 = 2J_1$ and $\Lambda_2 = 4J_2/d$, the saddle-point equations are

$$\Lambda + \Lambda_1 = \frac{1}{N} \sum_q \frac{1}{1/(\Lambda + \Lambda_1) + \Lambda/\Lambda_2 - \sum_{\mu=1}^{d} \cos q^\mu} \tag{7}$$

and

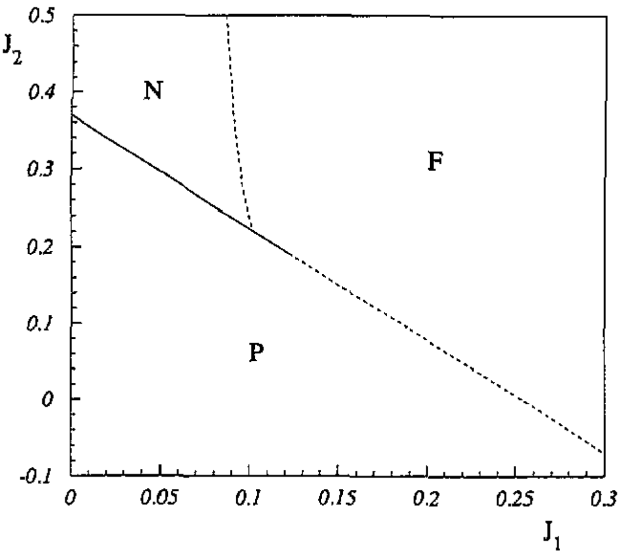

Figure 1. The phase diagram in $d = 3$. The full and broken curves represent first-order and critical transitions, respectively. The ferromagnetic, nematic and paramagnetic phases are indicated by F, N and P.

$$z = \frac{1}{2}\left(1 + \frac{\Lambda(\Lambda + \Lambda_1)}{\Lambda_2}\right). \tag{8}$$

Here the arbitrariness of $\mathrm{Re}\, z$ (and of $\mathrm{Re}\, A$ if $J_2 < 0$) is used to satisfy (7) and (8) with $\mathrm{Im}\, z = 0$ (and $\mathrm{Im}\, A = 0$ if $J_2 < 0$). For simplicity we will use the quantity Λ for distinguishing between the different phases; Λ is related to the nearest-neighbour correlation by

$$\frac{1}{n}\langle S \cdot S\rangle = \frac{\Lambda}{\Lambda_2 d}. \tag{9}$$

We first concentrate on the case $J_2 > 0$ in $d = 3$. Since at $\Lambda_1 > 0$ $\langle S_i \cdot S_j\rangle \geqslant 0$, equation (9) gives $\Lambda \geqslant 0$, so that (7) is well defined for $\Lambda > -\Lambda_1$ when $\Delta = (d\Lambda_2 + \Lambda_1)^2 - 4\Lambda_2 < 0$, or, if $\Delta > 0$, in the intervals $-\Lambda_1 < \Lambda \leqslant \Lambda_-$, $\Lambda_+ \leqslant \Lambda$, where $\Lambda_\pm = 1/2\big(d\Lambda_2 - \Lambda_1 \pm \sqrt{(d\Lambda_2 + \Lambda_1)^2 - 4\Lambda_2}\big)$ (corresponding to having no poles in the right-hand side of (7)). The right-hand side of (7) can be written as $\psi_d(\xi) = \int_0^\infty \mathrm{d}t\ \mathrm{e}^{-t(\xi+d)}[I_0(t)]^d$ [12], where I_0 is the Bessel function of zero order and $\xi = 1/(\Lambda + \Lambda_1) + \Lambda/\Lambda_2 - d$. At $\Lambda = \Lambda_\pm$ one gets $\xi = 0$ and $\psi_d(0)$ is finite for $d > 2$ ($\psi_3(0) = 0.5054$). Now we can comment on the phase diagram shown in figure 1. At small J_2, when J_1 is also small, $\Delta < 0$ and *there is only one solution of (7). On increasing J_1, Δ becomes positive, but only the right* branch of ψ_d ($\Lambda_+ \leqslant \Lambda$) gives a solution of (7). At still larger values of J_1, $\psi_d(0)$ becomes less than $\Lambda_+ + \Lambda_1$ and a solution can be found by extracting the zero mode in the sum of (7), as is usually done in the spherical model. Hence, there is a continuous transition at $\psi_d(0) = \Lambda_+ + \Lambda_1$, or

$$J_2^{\mathrm{crit}} = \frac{d\psi_d(0)^2}{4(d\psi_d(0) - 1)} - \frac{d\psi_d(0)}{2(d\psi_d(0) - 1)} J_1. \tag{10}$$

The situation is different at larger values of J_2—just before ψ_d splits into two branches, the maximum of the RHS of (7) is less than $\Lambda + \Lambda_1$. Then, for $\Lambda_1 > 2\sqrt{\Lambda_2} - d\Lambda_2$ ($\Delta > 0$), there is one solution of (7) due to the zero mode of the right branch of ψ_d, while two other solutions of (7) come out due to the left branch ($-\Lambda_1 < \Lambda \leqslant \Lambda_-$). The stable solution is the one minimizing (6). Here the transition is first-order. The tricritical point occurs when $\Delta = 0$ and $\Lambda_1 + \Lambda_+ = \psi_d(0)$. The two conditions are verified on the critical line at $J_2^{\rm tric} = 0.191$. When $J_1 = 0$, the results of [8, 11] are recovered .

When $J_2 < 0$, the inequality $\Delta > 0$ always holds and (7) has to be solved in the interval $-\Lambda_1 < \Lambda \leqslant \Lambda_+$, since $\Lambda_- < -\Lambda_1$. Here the mechanism of the continuous transition is effective and the critical line is still given by (10). Therefore, as in the mean-field phase diagram, for $J_2 < 0$, the disordered phase extends to $T = 0$.

A more physical characterization of the various regions of figure 1 would also need the knowledge of the behaviour of the quadrupolar order parameter $\langle S_i^\mu S_i^\nu - \delta_{\mu\nu}\rangle$. By introducing in (2) an external field for this order parameter and solving a related saddle-point equation [11], it comes out in a simple way that the quadrupolar transition coincides with the transition in Λ. However, as has been discussed before, an Ising transition is expected at large J_2. In this context, this transition can be recovered only at order $1/n$. At large J_2 the spins align along a particular direction and each vector can be written as $S_i = (\Pi_i, S_i^n)$, with the Π_i's representing small fluctuations with respect to the preferred direction and S_i^n being of any sign. Then the δ-functions in (2) can be written as

$$\delta\left(\frac{S_i^2}{n} - 1\right) = \frac{n}{2} \sum_{\tau_i=-1,1} \frac{1}{\sqrt{n - \Pi_i^2}} \delta\left(S_i^n - \tau_i\sqrt{n - \Pi_i^2}\right) \tag{11}$$

where the τ_i's are Ising variables defined at the sites of the lattice. Then the last component of S_i can be integrated out and to the lowest order in Π we get

$$\mathcal{Z} = \frac{n^{N/2}}{2^N} \frac{e^{dn NJ_2}}{(2J_2)^{(n-1)N/2}} \sum_{\{\tau_i\}} e^{nJ_1 \sum_{\langle ij\rangle} \tau_i \tau_j} \int \prod_i d\Pi_i \, e^{-\mathcal{H}_0} e^{-(J_1/4J_2)\sum_{\langle ij\rangle} \tau_i\tau_j (\Pi_i - \Pi_j)^2 + (1/4J_2)\sum_i \Pi_i^2} \tag{12}$$

where

$$\mathcal{H}_0 = d\sum_i \Pi_i^2 - \sum_{\langle ij\rangle} \Pi_i \cdot \Pi_j . \tag{13}$$

The Gaussian variables Π_i can finally be integrated out and an Ising model comes out with effective exchange interaction $\beta = nJ_1 - J_1(n-1)/4J_2 d$ with a transition at

$$J_1 \approx \frac{\beta_c}{n}\left(1 + \frac{1}{4J_2 d}\right) \tag{14}$$

where β_c is the transition point of the d-dimensional Ising model ($\beta_c = 0.2217$ in $d = 3$ [13]). Figure 1 shows the complete phase diagram in $d = 3$. The ferromagnetic–nematic transition given by (14) is also shown for $n = 3$.

Now we consider the case $d = 2$. The continuous transition cannot survive, due to the fact that, as in the spherical model, $\psi_2(0)$ is an infinite quantity. The resulting phase diagram is shown in figure 2. It exhibits a first-order line starting from the J_2-axis and ending with a critical point at $J_1 = 0.013$, $J_2 = 0.453$. The quadrupolar order parameter can easily be shown to be always zero; therefore there is no continuous symmetry breaking, in accord with the Mermin–Wagner theorem [14]. The $n \to \infty$ limit of the model (1) in $d = 2$ seems to be pathological in many respects. On the line $J_1 = 0$ the transition is signalled only by the behaviour of $\langle S_i \cdot S_j\rangle$ which is a quantity always equal to zero for n finite, due to the local gauge-invariance of the model (1) ($S_i \to \epsilon_i S_i$ with $\epsilon_i = \pm 1$). Thus the physical meaning of the transition line of figure 2 is also questionable for finite n.

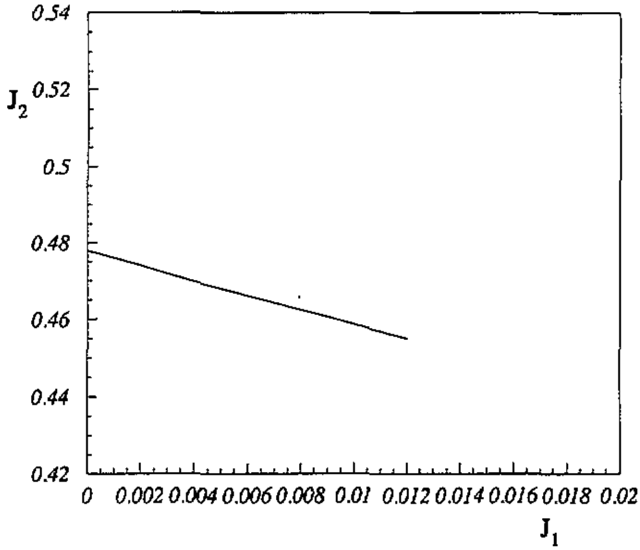

Figure 2. The first-order transition line in $d = 2$.

A realistic picture of the phase diagram of model (1) beyond the $n \to \infty$ approximation would be interesting to deduce. The $n = 2$ case needs further discussion. We know that at $J_2 = \infty$ there is an Ising transition, whereas at $J_2 = 0$ there is a topological transition at finite J_1 [15]. Therefore it would be interesting to know if the Ising critical point remains isolated or if it is stable moving inside the phase diagram and is related in some way with the critical point on the J_1-axis.

In summary, we have studied the phase transitions of an n-component spin model with dipolar and quadrupolar interactions at the leading order in the $1/n$ expansion. The resulting phase diagrams are shown in figures 1 and 2, and agree with mean-field results [1] and numerical simulations [4]. The nematic–ferromagnetic transition has been shown to be suppressed in the large-n limit.

One of us (GG) warmly thanks Mario Pellicoro for useful discussions. This work was supported by an NATO travel grant, an NSF MRG grant, INFN and by the Center for Academic Computing at Penn State.

References

[1] Krieger T J and James H M 1954 *J. Chem. Phys.* **22** 796
[2] Maier W and Saupe A 1956 *Z. Naturf.* A **13** 564; 1959 *Z. Naturf.* A **14** 822
[3] Chandrasekhar S 1992 *Liquid Crystals* (Cambridge: Cambridge University Press)
[4] Biscarini F, Chiccoli C, Pasini P and Zannoni C 1991 *J. Non-Cryst. Solids* **131** 1190; 1991 *Molec. Phys.* **73** 439
[5] Rodbell D S, Jacobs I S, Owen J and Harris E A 1963 *Phys. Rev. Lett.* **11** 10
Harris E A and Owen J 1963 *Phys. Rev. Lett.* **11** 9
[6] Lammert P E, Rokhsar D S and Toner J 1993 *Phys. Rev. Lett.* **70** 1650
Gonnella G 1994 *Phys. Rev.* E (at press)
[7] Thorpe M F and Blume M 1972 *Phys. Rev.* B **5** 1961
[8] Kunz H and Zumbach G 1989 *J. Phys. A: Math. Gen.* **22** 1043
[9] Berlin T H and Kac M 1952 *Phys. Rev.* **86** 821
[10] Stanley H E 1968 *Phys. Rev.* **176** 718

[11] Ohno K, Carmesin H O, Kawamura H and Okabe Y 1990 *Phys. Rev.* B **42** 10 360
[12] See, for example, Baxter R J 1982 *Exactly Solved Models in Statistical Mechanics* (London: Academic)
[13] See, for example, Domb C 1974 *Phase Transitions and Critical Phenomena* ed C Domb and M S Green (London: Academic)
[14] Mermin N D and Wagner H 1966 *Phys. Rev. Lett.* **17** 1133
[15] Kosterlitz L M and Thouless D J 1973 *J. Phys. C: Solid State Phys.* **6** 1181